

Traveltime computation through isotropic media via the eikonal equation

Marco A. Perez and John C. Bancroft

ABSTRACT

Traveltimes can be computed through a complex velocity structure by a finite-difference approximation to the eikonal equation. The main methods investigated here consist of the same finite-difference scheme yet differ in the order in which the points were computed. The first method estimates traveltimes along an expanding square while the second uses an expanding wavefront. Theoretically, it is expected that the expanding wavefront algorithm will be more accurate, however it takes more computational resources and time for computing the traveltimes. The expanding-square method is fast but is expected to suffer accuracy problems in complex structures. Deciding between the two methods is a trade-off between accuracy and computational time.

INTRODUCTION

Traveltime computations of waves propagating through different layers of isotropic media have been estimated with two basic methods. The first is raytracing, in which the path that the energy travels is computed from the invariance of the ray parameter. Many raytracing methods have been suggested, yet these all have problems that can be divided into two categories. The first problem is that in strongly varying velocity fields, there may be more than one raypath possible to reach a certain point. To ascertain the minimum traveltime, all these paths should be computed and compared, something that is quite tedious. The second is the problem of shadow zones. Shadow zones are areas in which rays cannot be found that pass through it. There is a specific angle, or finite number of angles, at which each ray must depart from the source to reach a certain point. At times, the position at which the ray ends is extremely sensitive to the angle of departure and finding the appropriate angle can be difficult.

Another method, which will be the focus of this discussion, calculates traveltimes through a finite-difference approximation to the eikonal equation. The methods that will be investigated here are those proposed by Vidale (1988) and by Qin et al. (1992). These methods do not have a shadow zone problem and their intent is only to search for the first-arrival traveltimes. A drawback of this method is that the path travelled may not always be obvious. The nature of the eikonal equation does not allow for travel path information to be propagated and hence is somewhat at a disadvantage compared to the raytracing methods.

Considerations discussed within the report include the computational time taken to calculate the traveltimes and accuracy. The raytracing methods can be quite expensive in comparison to the eikonal method because it does not have the problems encountered in the raytracing method. This report does not intend to advocate one

particular finite-difference method over another, but merely to point out differences between the methods that one should consider.

THEORETICAL ASPECTS

The finite difference scheme developed to compute traveltimes begins with the eikonal equation. Berkhout (1985) derives the eikonal equation from the wave equation and defines it as:

$$|\nabla\tau_i| = \frac{1}{c} \quad (1)$$

It provides traveltime information based only on the velocity which depends on position, i.e. $c=c(x,y,z)$. This equation can be used as an approximation for calculating the traveltime through an isotropic medium, if the velocity function is defined appropriately. This can be used to calculate traveltimes of P and S waves as they propagate into the Earth through a variety of different layers, each with their own unique properties.

The eikonal equation is solved with a finite-difference scheme proposed by Vidale (1988). Considering a two-dimensional model, Vidale expresses the eikonal equation as:

$$\left(\frac{\partial t}{\partial x}\right)^2 + \left(\frac{\partial t}{\partial z}\right)^2 = s(x, z)^2 \quad (2)$$

where s denotes slowness, the inverse of velocity. Though Vidale shows two approximations, one for a plane-wave approximation and the other for circular wavefronts, only the plane-wave approximation will be considered here. The two differential terms of equation (2) are approximated as:

$$\frac{\partial t}{\partial x} = \frac{1}{2h}(t_0 + t_2 - t_1 - t_3) \quad (3)$$

and

$$\frac{\partial t}{\partial z} = \frac{1}{2h}(t_0 + t_1 - t_2 - t_3) \quad (4)$$

where t_0 , t_1 , t_2 and t_3 are the corners depicted in Figure 1. In equations (3) and (4), h refers to the spacing between points in the discrete model. Combining these equations into equation (2), the resulting equation solved for t_3 yields:

$$t_3 = t_0 + \sqrt{2(hs)^2 - (t_2 - t_1)^2} \quad (5)$$

This equation allows for the solving of the traveltime at a specific point given the traveltimes of three surrounding points. Equation (5) is represented pictorially in Figure 1.

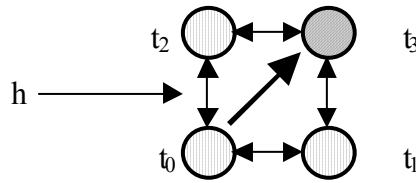


Figure 1. Finite difference illustration of equation (5), the 3-point equation. The double arrows denote distance h and thick arrow shows the raypath.

This equation will now be referred to in this discussion as the '3-point equation'.

The other equation used is referred to, within this paper, as the 'extrapolation equation'. In this case a non-centred finite difference scheme is used. Making a plane wave approximation the extrapolation equation is found to be

$$t_3 = t_0 + \sqrt{(hs)^2 - 0.25(t_2 - t_1)^2} \tag{6}$$

This formula also determines the traveltime to a specific point using 3 points; however, these points are located at different positions, as illustrated in Figure 2.

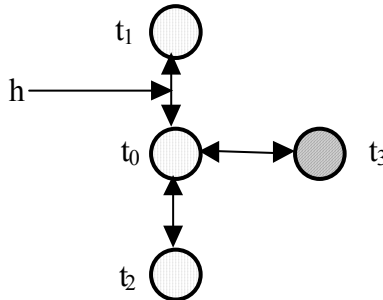


Figure 2. Finite-difference illustration of equation (6), the extrapolation equation. Double arrows denote the distance h .

As seen in Figures 1 and 2, the distance between each grid-point pair is constant, denoted by the distance h . If this were not the case, both the 3-point and the extrapolation equation would be more complicated. The final formula, which is used infrequently, is referred to as the 'simple equation' and has the form:

$$t = h \cdot s + t_0 \tag{7a}$$

where t is time, h is the distance travelled and s , is the slowness or the inverse of velocity.

The 3-point and extrapolation equation also ensue from simple geometry assuming plane waves. Consider the figure below.

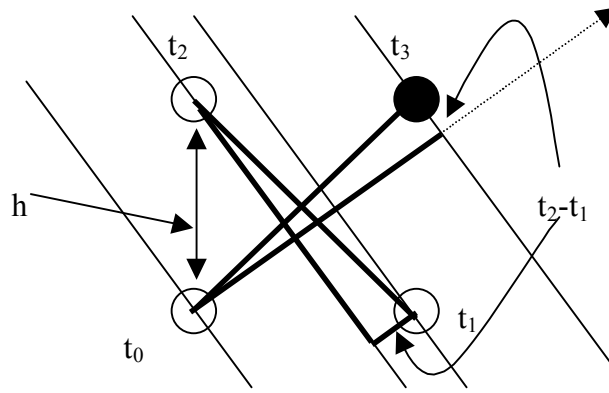


Figure 3. Plane-wave approximation to compute traveltimes for the 3-point equation.

The two triangles specified are identical and thus the respective sides of the triangles are of equal length. Both triangles have a hypotenuse length of $\sqrt{2}h$. The triangle, which has a side parallel to the wavefronts, also has a side that is the time difference t_2-t_1 . Because these are identical triangles, it follows that the time difference between t_3 and the ray perpendicular to the wavefront that passes through the point t_0 is also $t_2 - t_1$. Therefore knowing two sides, we can determine the third with the Pythagorean theorem:

$$2h^2 = \left(\frac{t_2 - t_1}{s}\right)^2 + \left(\frac{t_3 - t_0}{s}\right)^2 \quad (7b)$$

Solving for t_3 yields the 3-point equation (5). A similar construction is made for the extrapolation equation.

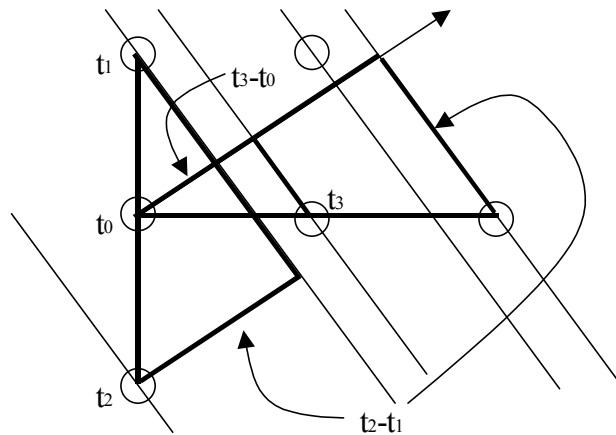


Figure 4. Plane-wave approximation to compute traveltimes for the extrapolation equation.

In Figure 4, two identical triangles are seen where one side is the time difference of t_2-t_1 . The triangle of interest is half the size of the two identical triangles. So, instead of using the quantity t_2-t_1 , only half the time difference is used. Using the Pythagorean theorem we have

$$\left(\frac{t_3 - t_0}{s}\right)^2 + \left(\frac{1}{2}\frac{(t_2 - t_1)}{s}\right)^2 = h^2 \quad (8)$$

Solving for t_3 yields the extrapolation equation. Thus equations (7b) and (8) have had the traveltimes computed using a plane-wave approximation and equal grid spacing.

PROPOSED METHODS AND ALGORITHMS

Method 1: Expanding-square method; Vidale (1988)

The algorithm begins from a source point, which will be denoted as point S . From this point S , the points, lying horizontally and vertically, are calculated using the simple formula, equation (7a), illustrated in Figure 5.

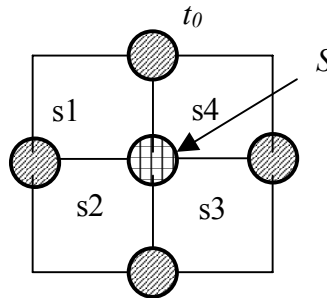


Figure 5. The four initial points calculated using the simple equation, starting from the source point S .

Notice that from the source point there are two velocities that a ray could take to reach a point. In travelling from the source point to point t_0 the wave could travel at a slowness of $s1$ or $s4$. In determining which path the ray would take, since we are only interested with the first arrival, the smaller slowness is used. In future diagrams the slowness grids will be omitted.

Following the computation of the initial traveltimes, the corner points are calculated using the 3-point equation.

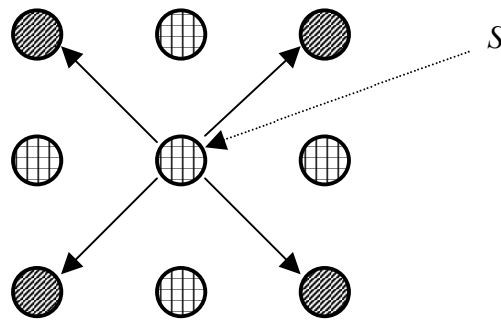


Figure 6. Corner points are computed using the 3-point equation. S denotes the source point.

Once the ring of 8 points is calculated, the main portion of the algorithm can be used. This consists of calculating traveltimes along each of the edges of the now expanding square. The right side of the square will be considered, yet the algorithm works in the same manner for all sides. Suppose that the square now has edges of 7 points. The first step is to determine the local maxima and minima of the calculated time at these 7 points.

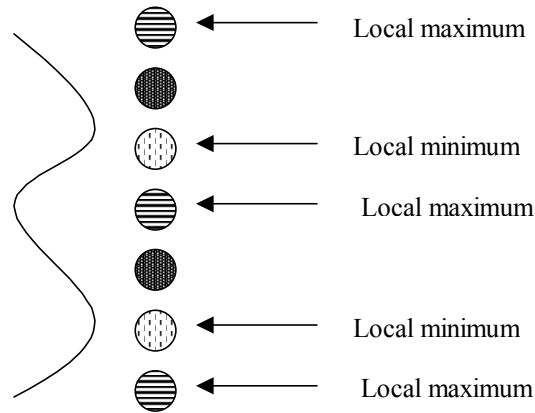


Figure 7. Determination of local maxima and minima along the edge of the square. Horizontal stripes denote a local maximum while the vertically-dashed lines denote a local minimum.

From the local minima the next point is calculated. It is assumed that as the wave expands it will reach the point directly in front of the local minimum first. This is because in an isotropic medium the raypath will be perpendicular to the wavefront and as such, at the minimums the ray will be pointing in the direction of the shortest distance to the next point. It is hoped that by following this scheme, causality will be followed. From the minima, the traveltimes at the next point is computed using the extrapolation equation. These new points are referred to throughout the algorithm as anchor points. This is illustrated in Figure 8.

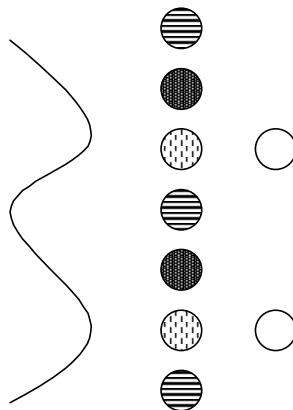


Figure 8. First step in expanding the square size. Anchor points are in white.

Once the traveltimes of these first points are computed on the new edge, the procedure is as follows. Using the 3-point equation one solves 'up' until a local maximum is reached (Figure 9).

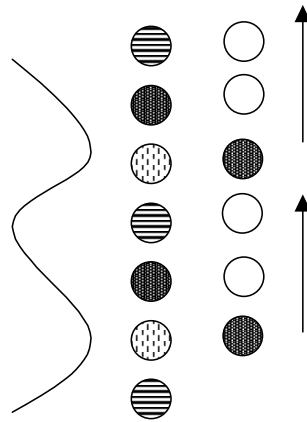


Figure 9. Second step in expanding-square edge.

Following this second step, from each of the ‘anchor’ points, one solves ‘down’ again using the 3-point equation (Figure 10).

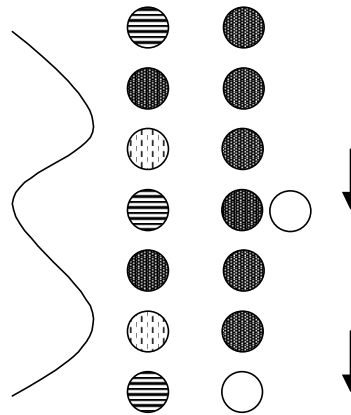


Figure 10. Third step in expanding-square edge. Notice that the fourth point from the bottom is solved twice. The minimum of the two estimated traveltimes is taken as the first arrival.

Finally in this manner all points along the new edge are computed. However, there is one point, the fourth point from the bottom, which is calculated twice. Keeping the minimum traveltime of these two calculations ensures that we are considering only the first arrival. This has only been shown for the right edge of the expanding square yet the same approach is taken for the remaining three edges. Note that in starting from the minima one hopes to avoid instabilities and follow causality.

The final step of expanding the square consists of calculating the corner points of the square. The last four points are calculated using the 3-point equation.

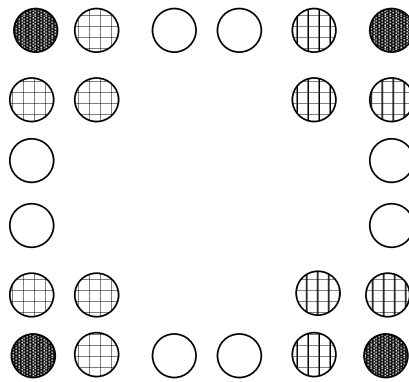


Figure 11. Dark points are corner points to be determined using the traveltimes information of the striped points. All other points in the square have been calculated.

This procedure is repeated until the traveltimes for the entire slowness grid has been calculated.

When implementing this algorithm, the user must recognize that a series of approximations have been made and that the accuracy of the method is a valid concern. The method, however, is simple and runs quickly, proportional to the number of points to be calculated.

Problems and possible solutions to the expanding-square method

The problem with the Vidale expanding-square algorithm is that it is not always appropriate for models with moderate-to-large velocity contrasts. This is because the method does not always follow causality. In other words, the times for the points leading up to a given point are unknown and thus the traveltimes calculation is not computed accurately. Since this algorithm expands in terms of grid points and not traveltimes, there are occasions when it can be noncausal. As a demonstration of this, consider the figure below.

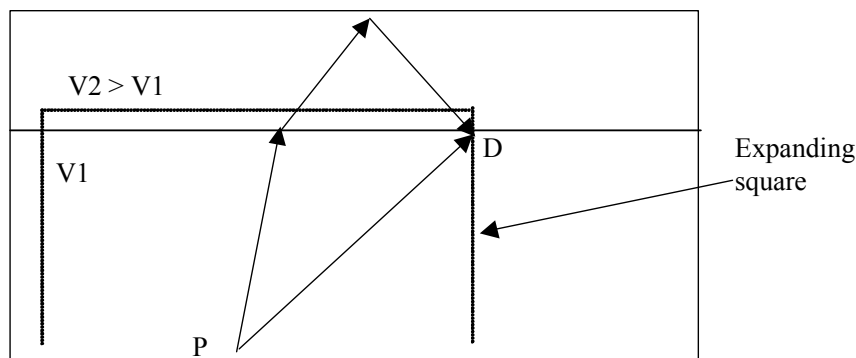


Figure 12. A ray emanating from point P may reach the point D, in less time travelling through the top layer. However, because of the expanding square, it will not have the traveltimes information to correctly determine the point D. V_2 and V_1 denote velocities.

In this case, two different routes can reach point D from P. However, since we are dealing with an expanding square, the times from the higher-velocity region will not

be taken into account when attempting to compute the traveltime at point D. Mathematically this transforms into having a negative in the square root of equation (5), the 3-point equation. Roughly speaking, the expanding square scheme violates causality if $V_2/V_1 > \sqrt{2}$ (Qin et al., 1992).

As a possible correction to the noncausal nature of the Vidale algorithm, consider the possibility of rays reaching a point via a different route shown in the figure below.

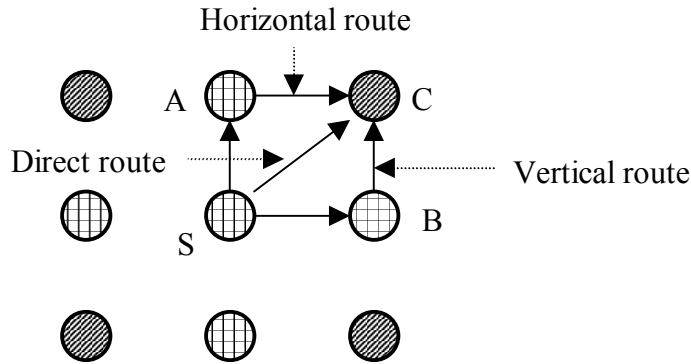


Figure 13. Possible different routes taken to reach corner points, which would take less time than the direct route: the horizontal and vertical route.

Here, the horizontal route of a wave from the source point passes through point A first. The vertical route is defined as the one which passes through point B on its way to the destination point C. This method of wave propagation is based on Huygens principle, which considers each point reached as a secondary source point. Zhu (1997) has also suggested this method. Within each route, there is a choice of which slowness grid the raypath will take.

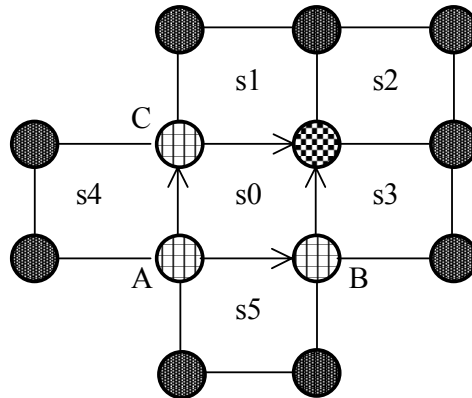


Figure 14. Slowness possibilities in determining the traveltime and path taken to the destination point (checkered). Dark points are unknowns while the striped points are known.

In Figure 14, the direct route simply uses the slowness s_0 and the 3-point equation. A wave taking the horizontal route first approaches point C, choosing along the way the minimum traveltime to reach this point, corresponding to selecting the minimum slowness between s_4 and s_0 and solving for the traveltime using the simple formula.

Once at point C, to reach the destination point (checked in Figure 14) in the least time possible, the smallest slowness is then also chosen between s_0 and s_1 and the traveltime computed again using the simple formula. Similarly, for the vertical route, point B is calculated using the simple formula and the minimum slowness between s_0 and s_5 and again from point B to the destination point taking the smaller slowness between s_0 and s_3 . Once these three routes are considered, the minimum traveltime of the three is chosen, corresponding to the first arrival. This alleviates the potential problem in equation (5). With a square root in the problem, there is a chance for imaginary numbers to occur. This occurs when sharp slowness contrasts occur at the boundaries. In such cases, the traveltime will be limited to choosing between the horizontal and the vertical route.

However there are problems in making such assumptions that can lead to inaccurate calculation of traveltimes.

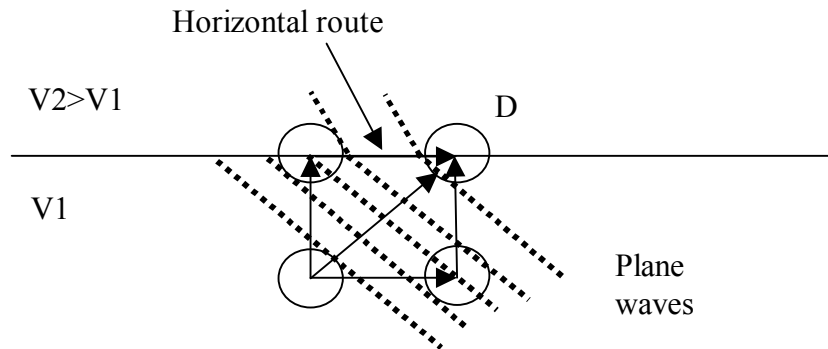


Figure 15. Traveltime inaccuracies in using the possible different routes. V_2 and V_1 are velocities

When using a plane wave approximation, the correct traveltime is computed with the 3-point equation even if it is possible that point D can be reached through the medium of velocity V_2 , the horizontal route. When using the simple equation, information of the plane wave trajectory is lost. Since Huygens principle should reconstruct the plane wave, the velocity used in the simple equation is different than the actual velocity of the medium. The proposed adaptation to Vidale's method allows the noncausal nature of the algorithm to be overcome at the expense of loss in accuracy.

Another possible way to correct for the Vidale algorithm's inability to compute traveltimes in a complex model is to smooth the velocity model. One way to smooth the velocity is to recompute it as the average of nine velocity areas. This is repeated three times in hopes of obtaining a Gaussian distribution of the average, a consequence of the central limit theorem. Through this smoothing, there will be a reduction in the large velocity contrasts between layers that produce the Vidale instabilities. However, this also changes the model and thus the traveltimes are a reflection of the new model and not the original. Since this is an approximation to the original model, the traveltimes are correspondingly not as accurate.

Method 2: Expanding-wavefront method; Qin et al (1992)

In this method, instead of an expanding square, the method attempts to approximate an expanding wavefront. In this way, the limitations of the Vidale algorithm are hopefully overcome.

Specifically, the algorithm begins with the source point as the only accepted point and proceeds with the calculation of the eight points surrounding the source point, considered as the first estimation zone. These points are computed using the same finite-difference scheme used in the Vidale algorithm. The minimum of the estimation zone is chosen and it is denoted as accepted and removed from the estimation zone. Then all points, which are not accepted, are estimated or re-estimated to construct a new estimation zone. The following figures illustrate this process.

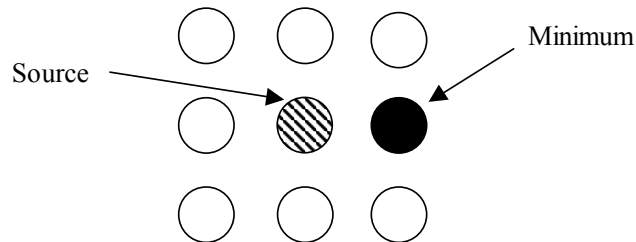


Figure 16. Source point surrounded by the first estimation zone. The first minimum of the estimation zone is the black point.

In determining the new estimation zone points, a specific order of computation is followed in relation to the minimum of the previous estimation zone. The reconstruction of the estimation zone begins with the vertical and horizontal points that have never been estimated before. All horizontal and vertical points are computed via the same extrapolation equation.

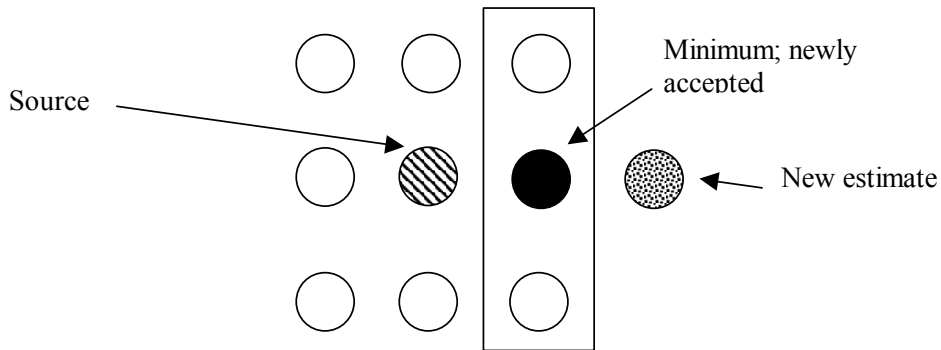


Figure 17. Points used to calculate the first new point of the new estimation zone via the extrapolation equation.

The remaining horizontal and vertical points, which are not accepted, are re-estimated.

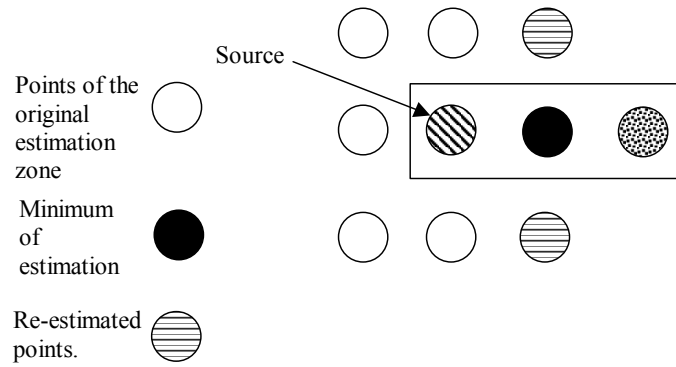


Figure 18. Re-estimation of points using the extrapolation equation or the 3-point equation.

This is done for all the horizontal and vertical points that are not accepted. It is now clear why there is a specific order in which the horizontal and vertical points are calculated; the new estimates must be computed before the re-estimated points to facilitate the use of the extrapolation equation. After calculating the re-estimates, the minimum of the two estimates (original and re-estimated) is kept within the new estimation zone. After the horizontal and vertical points are calculated, the diagonal points are estimated or re-estimated using the 3-point equation.

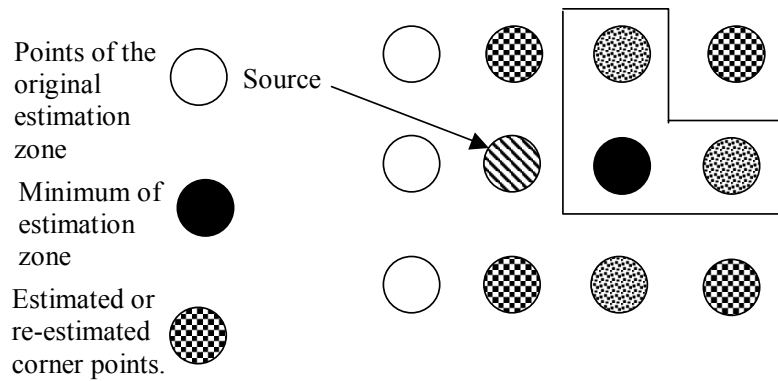


Figure 19. All corner points are estimated or re-estimated using the 3-point equation.

Finally, the new estimation zone is completely known from which a new minimum is chosen and the process repeated.

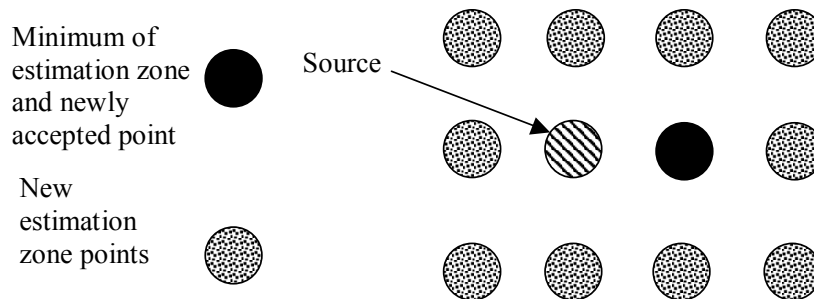


Figure 20. View of the estimation zone.

If the horizontal and vertical points are not calculated first, the 3-point equation cannot be used to estimate the corner points. Also, there is the elimination of the use of the simple formula, which is only used for the initial estimate of the horizontal and vertical points. Due to the waveform construction, the more accurate 3-point and extrapolation equations are used and, in the subsequent testing within this report, the instabilities seen in the original expanding-square algorithm are eliminated.

The pattern of (1) choosing the minimum from the estimation zone, (2) denoting it as accepted and (3) creating a new estimation zone, is repeated until all points in the model grid become accepted traveltimes points. This method is more accurate than the original and adapted Vidale algorithm, however, it must search through the estimation zone for the minimum and adds only one new accepted point per iteration, taking a larger amount of computational time.

APPLICATIONS AND RESULTS ON MODELS

Constant velocity model

Testing of the two methods begins with a constant-velocity model from where the exact traveltimes to all the points on the model grid can be exactly calculated. Figure 21 below, shows the results of the traveltimes computation for both the expanding square and wavefront method.

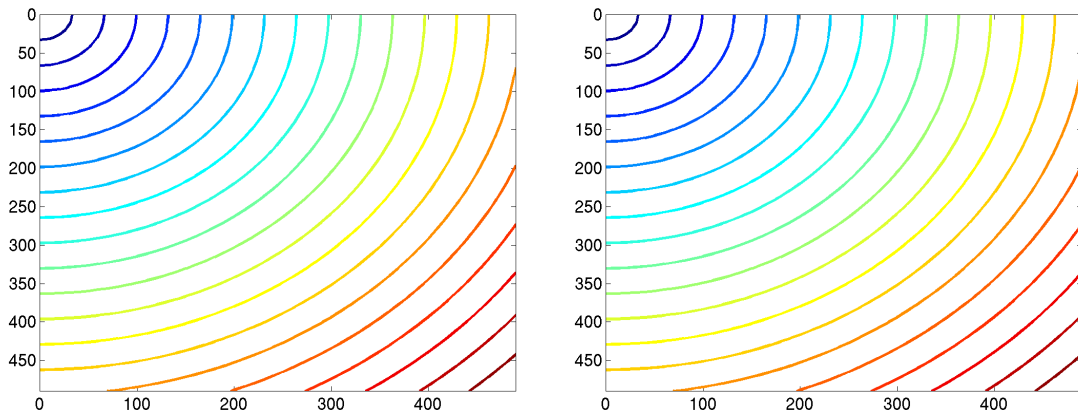


Figure 21. Constant velocity model traveltimes results of the expanding square (left) and expanding wavefront (right) methods. Figures have coordinates of metres along both the vertical and horizontal axes. Both plots have contour intervals of 0.0177.

Both the expanding square and wavefront method yield the same result. This is expected since the finite difference scheme used is the same in both methods and there are no harsh velocity contrasts. The error with respect to the exact results is shown below.

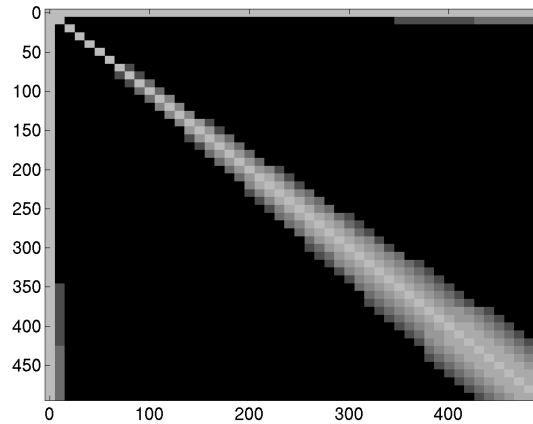


Figure 22. Error of the estimated traveltimes relative to the exact results. Black areas mean large error while grey shows little or no error. The axes have units of meters along both the vertical and horizontal axis.

The errors in this case are described as having a maximum value of 0.0007 with a mean of 0.0004 and a standard deviation of 0.0002 seconds. Notice that the error is small or zero for the lines, $x=0$, $z=0$ and the line of $x=z$. This corresponds to the area in which there is an accurate representation of the plane-wave approximation. For lines other than those mentioned, the circular curvature of the wavefront is approximated well, especially at small distances from the source. As the wavefront moves farther from the source, the accuracy of the calculation increases, because with an increase in distance from the source, the plane-wave approximation is improved. A method to increase accuracy is to use the circular-wave approximation in computing traveltimes as mentioned in Vidale (1988). This method includes solving a quartic equation and is beyond the scope of this report. Another possible method is to explicitly determine the traveltimes at small distances from the source until the plane-wave approximation becomes more legitimate. After constructing a larger source area explicitly, both algorithms are run with the results and error shown below in Figure 23.

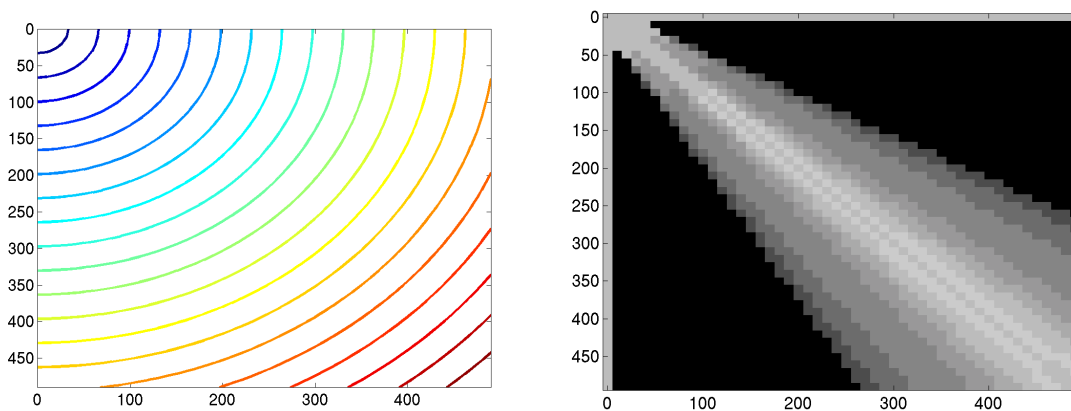


Figure 23. Result (left) and error (right) when using a source area instead of a source point. Units as in Figures 21 and 22.

The error in this case is described as having a maximum value of 0.0007 s, a mean of 0.0004 s and a standard deviation of 0.0002 s. These results are better as the errors at short distances are reduced after explicit calculation.

Linear velocity model

The next test is performed in another medium where traveltimes can also be calculated analytically. In a medium in which the velocity increases linearly, in the vertical direction, the traveltime from a source point on the surface to a point at depth, without reflection, is given by:

$$t = \left(\frac{1}{k}\right) \left(\cosh^{-1} \left(\frac{1}{\sin \theta} \right) - \cosh^{-1} \left(\frac{1}{\sin \theta_z} \right) \right) \quad (9)$$

where θ is the angle at which the ray departs from the source and θ_z is the angle at which it reaches the destination point. Also, for a ray in this medium that starts at the surface and ends at the surface, the traveltime is expressed as:

$$t = \left(\frac{2}{k}\right) \sinh^{-1} \left(\frac{kx}{2V_0} \right) \quad (10)$$

where x is the horizontal distance along the surface (Kleyn, 1983). Given these formulas and the corresponding linear velocity description of $V = V_0 + kz$, where V_0 is the velocity at the surface, k is the rate at which the velocity increases with depth and z is the depth of the point, the traveltimes to any point can be computed exactly. The velocity model to be used has parameters of $V_0 = 3000$ m/s and $k = 10$ s⁻¹. The model will be a discrete approximation to the continuous case, and with finer grid spacing the better the approximation. Using a grid spacing of 10 m, the results of using both the expanding-square and expanding-wavefront methods are shown below.

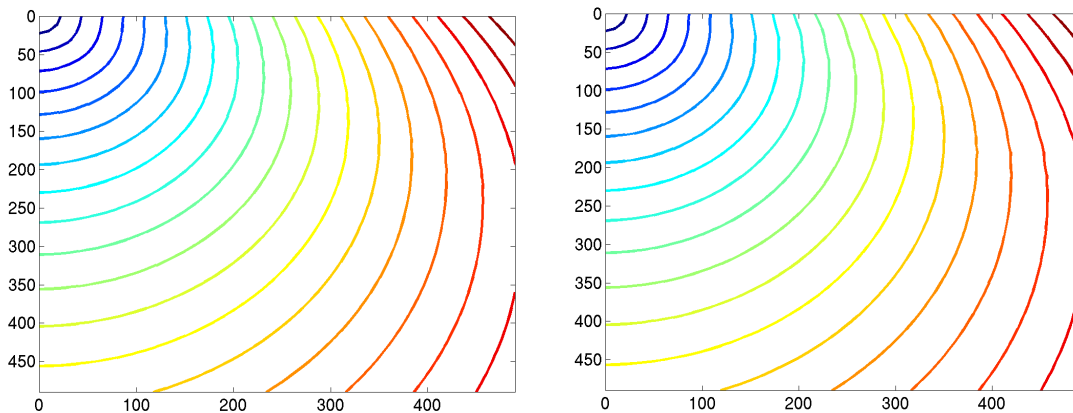


Figure 24. Calculation of traveltimes from a linearly increasing velocity model using the expanding square (left) and expanding wavefront (right) methods. Units as in Figure 21. Plot on the left has contour interval of 0.0076 ms and plot on right has contour interval of 0.0075 ms.

Notice that since the boundaries are smooth and continuous, the differences between the two methods should not be noticeable. The absolute errors are shown in Figure 25.

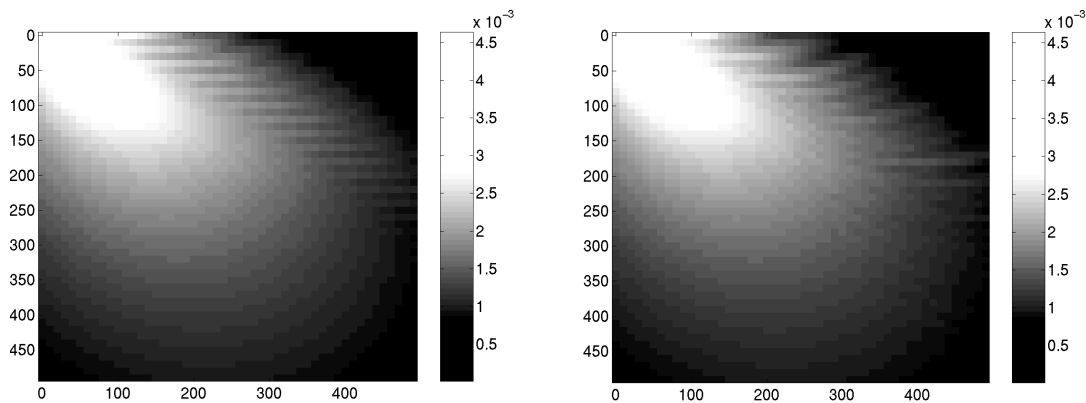


Figure 25. Errors of the calculation of the traveltimes using a linearly increasing velocity model from the expanding square (left) and expanding wavefront (right) methods. Units as in Figure 21. Large errors are denoted in white, small errors in black.

The error associated with the expanding-square algorithm has a maximum value of 0.0046 s and a mean of 0.0015 s. The expanding-wavefront method also has a maximum of 0.0046 s but a mean of 0.0014 s. The largest error corresponds with the locations of greatest curvature of the wavefront, the line $x=z$. There is also error along the $x=0$ and $z=0$ lines due to the discrete approximation to the continuous linear velocity model. The construction of the wavefronts more correctly as the distance increases is apparent in both error plots, a consequence of the plane-wave approximation.

Two final models

The last two models to be investigated consist of a qualitative analysis, since exact traveltimes are extremely difficult to compute. Raytracing could be used to compare between algorithms but this is not investigated here. We begin with a five-layer model shown in Figure 26 below.

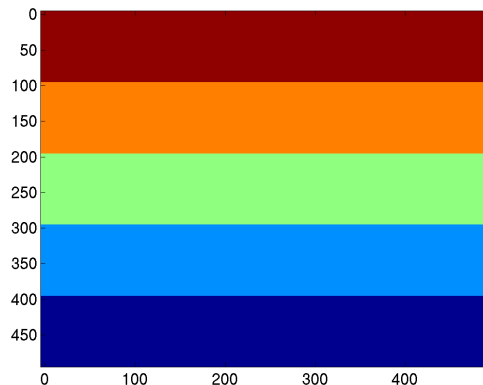


Figure 26. 5-layer model in which each layer increases in velocity with depth.

The velocities for the five layers increase in depth by 1000 m/s starting at 1000 m/s and ending at 5000 m/s. Notice that the first two layers have a velocity ratio of 2, which is greater than the limit of $\sqrt{2}$ beyond which the Vidale algorithm does not work and the algorithm produces imaginary numbers. The results of the expanding-square and expanding-wavefront methods are shown in Figure 27.

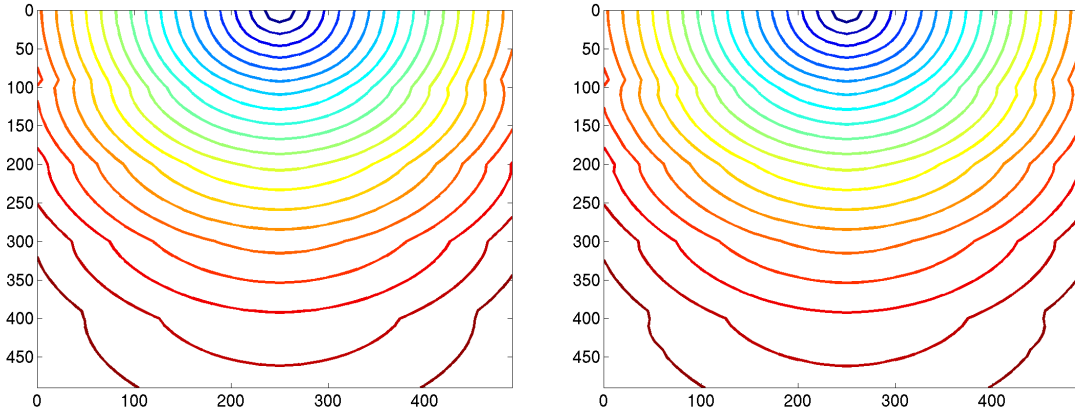


Figure 27. Traveltime contours of the 5-layer velocity model using the expanding-square (left) and expanding-wavefront (right) methods. Units as in Figure 21. Contour interval of 0.0810 s for plot on the left and of 0.0808 s for plot on right.

Both methods exhibit traveltime contours that show results that are reasonable. The differences between these two estimates are shown below in Figure 28. The differences arise from the manner in which the boundaries are handled.

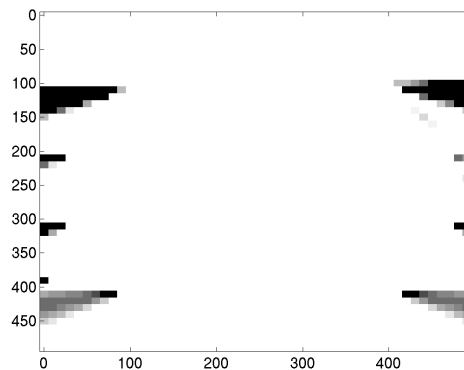


Figure 28. Difference between the expanding-square and the expanding-wavefront methods in the 5-layer model.

The next model has two layers with a velocity ratio of 3 between the higher velocity and the lower velocity. The model is shown below in Figure 29, followed by the results using the adapted expanding square and expanding wavefront algorithm.

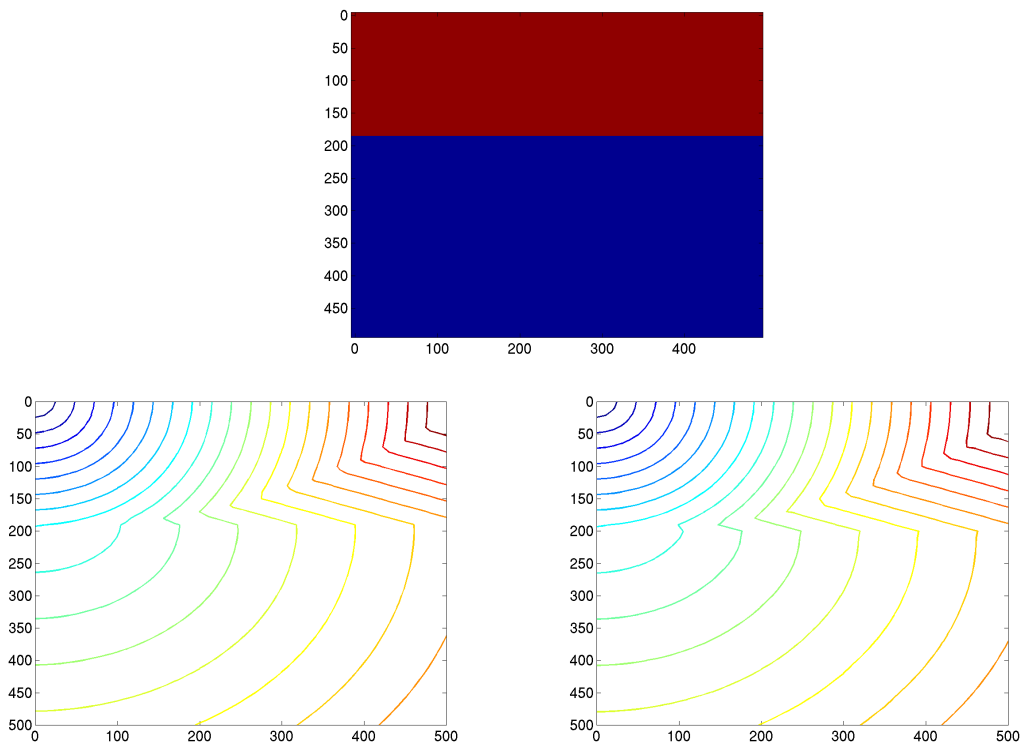


Figure 29. Two-layer model with a velocity ratio of 3 (top) with traveltime contours using the expanding-square (bottom left) and expanding-wavefront (bottom right) methods. Units are the same as in Figure 21. A contour interval of 0.0250 was used for the plot on bottom left and 0.0246 for plot on the bottom right.

Both results are similar and reasonable. The figure below indicates that the differences in the algorithms affect the manner in which the refraction is handled.

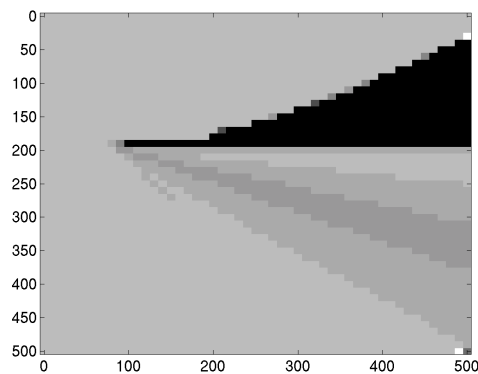


Figure 30. Differences between the expanding-square and the expanding-wavefront methods in the two-layer velocity model.

Due to the inaccuracy problems from the adapted Vidale algorithm, especially in boundaries with large velocity contrasts, the wavefront construction method of Qin et al. (1992) is expected to result in more accurate traveltimes. Still, it is surprising how well the assumptions made in the adapted Vidale algorithm come close to the expanding-wavefront method.

DISCUSSION

In comparing the three algorithms that have been implemented, we can easily discard the original Vidale algorithm. For all practical purposes, this original Vidale algorithm is not useful for a large variety of velocity models, even those that are only moderately complex. Essentially, the comparison of methods involves only the adapted Vidale algorithm, or the expanding-square algorithm and the expanding-wavefront technique proposed by Qin et al. (1992).

The expanding-square method is fast and with the few modifications made can handle any velocity model. However, it is expected to have some accuracy problems. Though the original instabilities of the Vidale algorithm have been overcome, the method in which this was done does not always take into consideration the direction in which the plane wave is travelling. It is because of this that, when dealing with a complex model, the results should be viewed critically.

The expanding-wavefront method is expected to be more accurate. A test with the linearly increasing velocity model complies with this expectation. The increase in accuracy requires an increase in computing time. The work by Qin et al. (1992) suggests methods to improve the efficiency of the expanding-wavefront method. Further research should continue to address this problem in order to make this method more efficient.

CONCLUSION

The finite-difference approximation to the eikonal equation method addressed in this discussion yields results that are accurate in the constant-velocity and linear-velocity models, as well as reasonable for the more complex velocity models. In terms of accuracy, there was no meaningful difference between the errors of the two methods in the cases where analytical traveltime solutions were computed. It is expected that, as the velocity model becomes more complex, the greater the difference will be between the expanding square and the expanding wavefront method. Further testing is required to determine the validity of this statement.

An inclusion to the expanding wavefront and square algorithms could be the circular-wavefront assumption into the traveltime computation. This would hopefully alleviate the errors at short distances from the source, a consequence of the plane-wave approximation.

Determining the accuracy in complex models is still something that needs to be done to truly produce concrete results. However, given the results from the testing performed so far, it appears that there is not much gained in choosing the more accurate, yet more time-consuming expanding-wavefront algorithm.

ACKNOWLEDGEMENTS

The authors would like to acknowledge the CREWES sponsors as well as the help and useful discussions of the following people: Dr. Gary Margrave, Dr. Larry Lines and Xinxiang Li of Sensor Geophysical Ltd.

REFERENCES

- Berkhout, A.J., 1985, Seismic Migration: Imaging of acoustic energy by wave field extrapolation A. Theoretical aspects, Elsevier, New York.
- Kleyn, A.H., 1983, Seismic Reflection Interpretation, Elsevier Applied Science Publishers, New York.
- Qin, F., Luo, Y., Olsen, K.B., Cai, W., and Schuster, G.T., 1992, Finite-difference solution of the eikonal equation along expanding wavefronts: *Geophysics*, 57, 478-487.
- Vidale, J., 1988, Finite-difference calculation of travel times: *Bulletin of the Seismological Society of America*, 78, 2062-2076.
- Zhu, J., 1997, Practical Imaging of complex geological structures using seismic prestack depth migration, Ph.D. Thesis, Memorial University of Newfoundland, St John's Newfoundland.